[November, 1977] BULLETIN OF THE CHEMICAL SOCIETY OF JAPAN, VOL. 50 (11), 2831—2836 (1977)

On the Behavior of Paramagnetic Species Formed in the Pure V_2O_5 Crystal under SO_2-Oxidation

Yoshiya Kera and Keiji Kuwata

Department of Chemistry, Faculty of Science, Osaka University, Toyonaka, Osaka 560

(Received March 10, 1977)

Two types of ESR spectra were found in the highly purified V_2O_5 crystal under conditions of SO_2 oxidation. The shapes and the intensities of the spectra were investigated in detail in the temperature range from 470 to 656 °C under various mixing ratios of SO_2 to O_2. Below *ca.* 600 °C a sharp and asymmetric spectrum existed stably, while above that temperature it was replaced by a spectrum with an hfs of 29 lines, the intensities of which always were very weak. The low-temperature-type spectrum was reasonably assigned to the $VOSO_4$ phase, and the high-temperature-type, to an oxygen defect surrounded equivalently by four vanadium ions in the V_2O_5 phase. The interchange between the two spectra near 600 °C occurred reversibly and was related favorably to the following process in the surface layer of the V_2O_5 crystal: $2VOSO_4=V_2O_5+SO_3+SO_2$. The change in the working states of a pure V_2O_5 crystal according to the conditions of SO_2 oxidation was discussed.

There have been numerous reports[1–10] on the mechanism of SO_2 oxidation over vanadium oxide catalysts, which are used in the states of a fused mixture of V_2O_5 with alkali sulfates and of a mixture supported on silica and alumina gels. Many authors[5–10] have determined the changes in the mechanisms of SO_2 oxidation over the catalysts at around 450 °C; they have been discussed mainly from the point of view of reaction kinetics. Mastikhin *et al.*[11] have observed the ESR spectra of $V_2O_5 \cdot 3.5\,K_2S_2O_7$ supported on alumina gel during SO_2 oxidation and have suggested that the changes in the kinetics are related to some changes in the working states of the catalyst. However, no full solution to this problem has yet been given for multicomponent catalysts because of the complicated changes in the ESR spectra according to the reaction conditions.

In the highly purified V_2O_5 crystal, however, simple spectra were found under the conditions of SO_2 oxidation. The shapes and the intensities of the spectra showed clear changes depending upon the SO_2/O_2 ratio and the reaction temperature. The purpose of this paper is mainly to give proper assignments to the paramagnetic species and to discuss in detail the behavior of the species on the surface of the pure V_2O_5 crystal depending on the conditions of SO_2 oxidation.

Experimental

Materials. The V_2O_5 powder, which has been obtained by the decomposition of NH_4VO_3 (Special grade, Wako Pure Chem. Ind. Co.) was further chemically purified according to the methods of McCarley *et al.*[12] and Haemers.[13] The V_2O_5 single crystals were prepared by a zone-melting method with a Pt-boat. The crystals were cut into a proper size for contact with the reaction gases and for the ESR measurements. The $VOSO_4 \cdot 3H_2O$ (Special grade, Mitsuwa Chem. Ind. Co.) was used without further purification for the observation of the changes in the ESR spectra by dehydration and sintering.

Procedures. The V_2O_5 single crystal was placed in a quartz tube with an inner diameter of 0.3 cm and a length of 3 cm, which was connected by a gradual joint to a glass tube 0.6 cm in inner diameter. After pretreatment at 500 °C under evacuation for 1 h, it was cooled to room temperature. A given amount of a gaseous mixture of SO_2 and O_2 was introduced into the sample tube, and then the tube was sealed off. The reaction was carried out by heating the sample tube in an electric furnace for a long time. It was quenched by immersing it quickly in cold water before the ESR measurement. The procedure was repeated at various temperatures between 470 and 656 °C, the temperature fluctuation being kept within ±1 °C. The reaction conditions are summarized in Table 1.

Table 1. Experimental conditions of SO_2 oxidation on V_2O_5 crystal

Sample	SO_2 Torr[a]	O_2(air) Torr	SO_2/O_2 ratio	V_2O_5 mg	Volume cm^3
S_s-1	370	40(200)	9	29	4
S_s-2	375	34(170)	11	45	25
S_s-3	480	6(31)	80	32	25
S_s-4	556	0	∞	18	5

a) 1 Torr$=1.334\times10^2$ Pa.

The dehydration of $VOSO_4 \cdot 3H_2O$ and its sintering were done in the same ESR sample tube described above.

ESR Measurements. The ESR spectra were recorded at room temperature and at 77 K with an X-band spectrometer. The modulation frequency of the magnetic field was 455 kHz. The frequency of the microwave was determined to be 9326 MHz by the use of a wave meter. The calibration of the static magnetic field was done with DPPH and the Mn(II) ion doped in MgO as standards.

Determination of Spin Concentration. The spin concentration was determined with a single mode cavity (T_{011}) by the use of $CuSO_4 \cdot 5H_2O$ (single crystal) and DPPH (benzene soln) as the primary and the secondary standards of the spin concentrations respectively. A capillary tube which contained

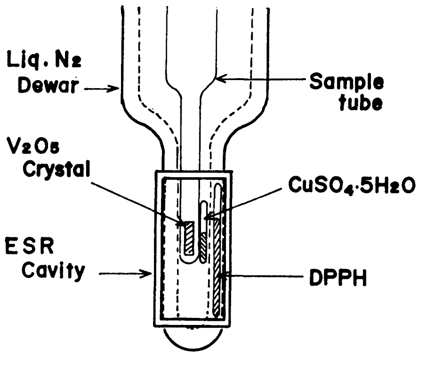

Fig. 1. Arrangement of V_2O_5 crystal and DPPH and $CuSO_4 \cdot 5H_2O$ standards in ESR cavity.

DPPH was always fixed on the outer wall of the quartz Dewar. On the other hand, a capillary tube which contained the $CuSO_4 \cdot 5H_2O$ was placed on the outer wall of the sample tube and was immersed together with it in the Dewar. The arrangement of the sample and the standards in the cavity are shown schematically in Fig. 1. The $CuSO_4 \cdot 5H_2O$ crystal was placed in the capillary tube so as to make the $g_{//}$ and $g_{\perp}$ axes nearly parallel to H_0 during the rotations of the sample tube around the axes. The spin concentrations were mainly obtained by a comparison of the integrated intensities of the standards with those of the samples. In the case of low spin concentrations, the amplitude of the first derivative curve of DPPH was used as a secondary standard.

Results

ESR Spectra in a Single Crystal of Highly Purified V_2O_5 under the Conditions of SO_2 Oxidation. No ESR signal was observed in the single crystal prepared from the cautiously purified V_2O_5 powder in air by the zone-melting method, although the signals ascribed to both vanadium ions (IV) with hfs of 15 lines and to the Fe ion as an impurity were usually found in the spectrum of the unpurified crystal. When the purified V_2O_5 single crystal was placed in contact with a gaseous mixture of SO_2 and O_2, an ESR spectrum with hfs of 15 lines and an hf-splitting constant, $A_{//}$, of 8.8 mT appeared initially. The spectrum is probably the same as has been found in pure and doped V_2O_5 by many authors,[14–16] as has been mentioned below. On prolonged contact the spectrum was replaced by an asymmetric spectrum, and the intensity of new spectrum increased with the time. When the temperatures were raised above *ca.* 600 °C, the asymmetric spectrum abruptly disappeared and a new spectrum with hfs whose splitting constant, $A_{//}$, is about 4.3 mT appeared. The former will hereafter be called the low-temperature-type spectrum, and the latter, the high-temperature-type spectrum.

In Run S_S-4, in which the crystal was treated at 617 °C with SO_2 alone, the spectrum with an hfs of 15 lines appeared initially, but soon disappeared. By this time the brilliance of the surface and the transparency disappeared completely, and the surface was covered with black and velveteen polycrystallines. Except for Run S_S-4, the surface brilliance of the cleaved plane (010) did not vary clearly upon the repetition of the heating and cooling, although the color and the transparency of the crystal did change.

Low-temperature-type Spectrum. The growth of the sharp asymmetric spectrum on Sample S_S-2 during the contacts at 470 °C is illustrated in Fig. 2. The line shapes of the asymmetric spectra at $H_0//b$ and $H_0 \perp b$ in Fig. 2 seem to show a typical randomly oriented paramagnetic species with an axially symmetric g-tensor. In the intermediate direction between $H_0//b$ and $H_0 \perp b$, however, an additional sharp line appeared in the asymmetric spectrum. The sharp line moved from the static magnetic field (position) corresponding to $g_{//}=1.924$ to that corresponding to $g_{\perp}=1.970$, according to the change in the direction of the static magnetic field from $H_0//b$ to $H_0 \perp b$ in the ac-plane. In a previous paper,[17] the angular dependencies of the spectrum were examined in detail and it was concluded that the asymmetric sharp spectrum was as a composite: one component was ascribed to the spectrum caused by an axially symmetric g-tensor ($g_{//}=1.924$ and $g_{\perp}=1.970$) taking a relatively random orientation to the crystalline lattice of the V_2O_5 and the other, to that taking a definite orientation, *i.e.*, the $g_{//}//b$-axis of the V_2O_5 crystal.

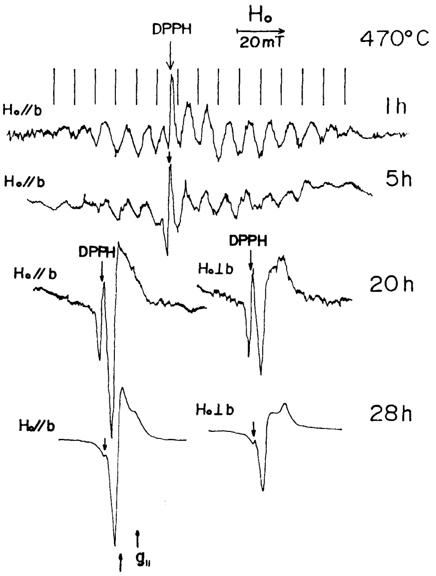

Fig. 2. Changes in ESR spectrum of a highly purified V_2O_5 single crystal during contact with a reaction mixture of SO_2 and O_2 at 470 °C.—Appearance and disappearance of ESR spectrum with hfs of 15-lines and then appearence of a sharp asymmetric spectrum (the so-called low temperature type spectrum).

Table 2. Changes in spectrum and its spin concentration in sample S_S-1 with the temperature

Temp °C	Time h	Low-temperature type Spin concn $\times 10^{17}$/29 mg	High-temperature type
505	134	8.2	—
639	43	4.7	—
656	17	0.7	hfs 29 lines
656	39	—	hfs 29 lines (4×10^{15})
599	166	3.8	—
549	163	6.8	—
532	70	6.6	—

The changes in the spin concentrations according to the reaction conditions are given for Samples S_S-1, S_S-2, and S_S-3 in Tables 2, 3, and 4 respectively. All the data were also graphically shown together in Fig. 3. In the case of Sample S_S-2, the time responses for the appearance and disappearance of the low-temperature-type spectrum are given in Fig. 4. It may be seen from the figures that the appearance and disappearance occur abruptly within the temperature range between 586 and 595 °C.

High-temperature-type Spectrum. At higher temperatures the low-temperature-type spectrum was re-

Table 3. CHANGES IN SPECTRUM AND ITS SPIN CONCENTRATION IN SAMPLE S_s-2 WITH TEMPERATURE

Temp °C	Time h	Low-temperature type Spin concn $\times 10^{17}$/45 mg	High-temperature type
470	229	1.5	—
536	166	4.5	—
595	96	0.1	hfs of 29 lines
640	65	0.08	hfs of 29 lines
586	161	5.2	—
513	180	6.2	—
481	230	8.9	—

Table 4. CHANGES IN SPECTRUM AND ITS SPIN CONCENTRATION IN SAMPLE S_s-3 WITH TEMPERATURE

Temp °C	Time h	Low-temperature type Spin concn $\times 10^{17}$/32 mg	High-temperature type
600	45	0.013	—
656	70	0.022	hfs 29 lines
481	167	0.32	—
550	161	0.97	—
572	160	1.1	—
516	180	1.1	—
476	228	4.6	—

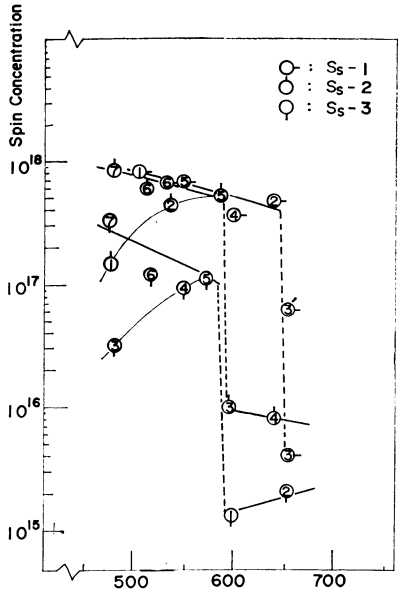

Fig. 3. Temperature dependences of spin concentrations of V_2O_5 single crystals after any periods of the contacts with SO_2+O_2 gases. The concentrations mean the numbers of unpaired electron per weight of used crystal. The figures in the circles indicate sequences of the measurements. Contact conditions are given in Table 1. The spin concentrations, the contact periods and sequences are given in Tables 2, 3, and 4, correspond to S_s-1, S_s-2, and S_s-3, respectively.

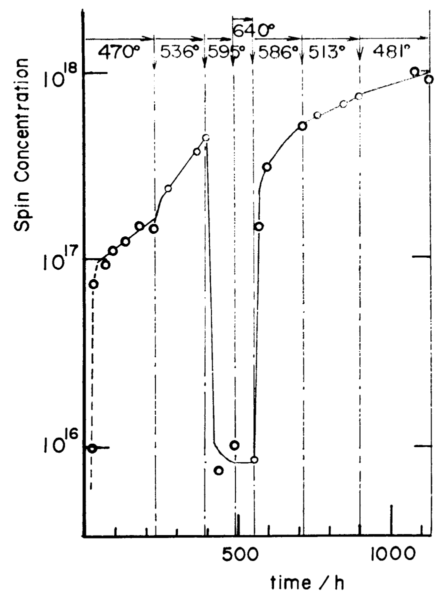

Fig. 4. Changes in the spin concentrations of the crystal, S_s-2 at various temperatures with the contact times.

placed by a new spectrum with hfs of more than twenty lines, whose hf-splitting constant was a half of that of the previous spectrum ($A_{//}=4.3$ mT). Such a change in the spectrum of Sample S_s-1 is illustrated in Fig. 5.

ESR Spectrum of Pure Vanadium Sulfate Powder. In mixtures of V_2O_5 and alkali sulfates under the reaction conditions of SO_2 oxidation, quite similar spectra with low-temperature-type spectra have been reported and ascribed to some states of vanadium sulfates.[11] The ESR spectrum of pure vanadium sulfate was also examined. The ESR spectrum of $VOSO_4 \cdot 3H_2O$ and the spectra obtained after heating $VOSO_4 \cdot 3H_2O$ in air at 490 °C for 24 h and then at 600 °C for 1 h are shown in Fig. 6. The higher the temperature, and the longer the treatment, the sharper and the more asymmetric the line shape. The *g*-values of the spectra are summarized in Table 5. In the limiting case we could obtain the spectrum with a *g*-value similar to that of the low-temperature-type spectrum. Upon heating at 620 °C the sharp asymmetric spectrum disappeared completely.

Discussion

High-temperature-type Spectrum in V_2O_5 Crystal under the Conditions of SO_2 Oxidation. There have been many reports on the ESR spectra of doped and undoped V_2O_5 single crystals. For instance, the spectrum with an hfs of 15 lines was found in Fe-, V-, and Cu-doped crystals,[14,15] and that with an hfs of 29 lines in Li- and Na-doped crystals.[20] In undoped V_2O_5 single crystals, spectra with hfs of 15 and 29 lines[16,18] were also reported; the spectra were ascribed to some kinds of oxygen vacancies in the crystalline lattices. No clear differences in the spectra with an hfs of 15 lines can be found between the doped and undoped crystals so long as only the ESR parameters are compared.

These results indicate that the hf-coupling constants

TABLE 5. COMPARISONS OF ESR PARAMETERS WITH RESPECT TO THE LOW TEMPERATURE TYPE SPECTRUM

Sample	Measurement Temp/K	$g_{//}$	$g_{\perp}$	$\langle g \rangle$	Reference
$V_2O_5 \cdot 3.5K_2S_2O_7$ on α-Al_2O_3 in working states	673	1.920	1.980	1.960	11
$VOSO_4$ on silica gel	300	1.915	1.969	1.951	19
V_2O_5 crystal in the SO_2 oxidation	77	1.924	1.970	1.955	The present work
$VOSO_4 \cdot 3H_2O$ powder	77	—	—	1.980	The present work
$VOSO_4 \cdot 3H_2O$ glyceline soln	77	1.940	1.990	1.973	The present work
$VOSO_4 \cdot 3H_2O$ heated in air at 148 °C for 4 h	77	1.929	1.967	1.954	The present work
$VOSO_4 \cdot 3H_2O$ heated in air at 490 °C for 24 h	77	1.932	1.970	1.957	The present work
$VOSO_4 \cdot 3H_2O$ heated in air at 600 °C for 1 h	77	1.925	1.966	1.952	The present work

TABLE 6. COMPARISONS OF ESR PARAMETERS WITH RESPECT TO THE HIGH-TEMPERATURE-TYPE SPECTRUM (at 77 K)

Sample	No. of hfs -line	$g_{//}$	$g_{\perp}$	$A_{//}$ (mT)	$A_{\perp}$ (mT)	Reference
Doped V_2O_5 crystal Fe-doped	15	1.82	1.98	10.5	5.0	14
Cu-doped	15	1.92	1.985	8.6	—	15
V-doped	15	1.92	1.991	9.0	3.7	15
Undoped	15	1.911	1.983	8.8	3.3	16
V_2O_5 crystal	29	1.931	1.982	4.3	—	18
S_8-1 (at 656 °C)	29	1.917		4.3	—	The present work
S_8-2 (at 470 °C, initially)	15	1.924		8.8	3.3	The present work

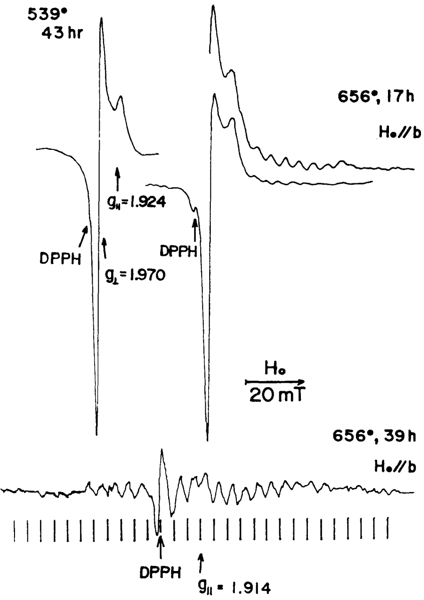

Fig. 5. Low temperature type spectrum at 539 °C, and disappearance of the spectrum and appearance of a new spectrum with hfs of more than 20 lines by the contact at 656 °C (the so-called high temperature type spectrum).

are related inversely to the number of ^{51}V nuclei, interacting equivalently with an unpaired electron, and thus to the number of the hf-lines, as has previously been suggested by Ioffe and Patrina.[14] According to such a rule, the spectrum with an hfs of 15 lines ($A_{//}$= 8.8 mT) in Fig. 2 can be ascribed to an oxygen vacancy of the Gillis type.[16] The high-temperature-type spectrum with the hf-splitting of 4.3 mT at $H_0//b$ in Fig. 5 could also be identified with the spectrum with an hfs of 29 lines,[18] although not all the hf-lines appear and the relative intensities of the hf-lines do not accord with a polynomial distribution. The lack of the full number of hf-lines and the correct intensity distribution might be caused by the relatively low concentration and the small fluctuation in the orientations of the paramagnetic species in the surface layer. Such a low concentration could be understood by thermochemical considerations, as will be mentioned below, and such a fluctuation in the orientations could be expected for the sample quenched from a real working state of SO_2-oxidation.

The positions of the hf-lines, however, were explained well by the following procedure and ESR parameters. Including the magnetic hyperfine interaction to the second order, the resonance field is given approximately by Eq. 1:[21]

$$\begin{aligned} H(m_I) = H_0 - Km_I/g\beta - (4H_0)^{-1}\cdot(g\beta)^{-2}\cdot A_{\perp}{}^2\cdot(A_{//}{}^2+K^2)K^{-2}\cdot \\ \{I(I+1)-m_I{}^2\} - (2H_0)^{-1}\cdot(g\beta)^{-2}\cdot \\ (A_{//}{}^2-A_{\perp}{}^2)K^{-2}\cdot g_{\perp}{}^2\cdot g_{//}{}^2\cdot g^{-4}\cdot z^2(1-z^2)m_I{}^2, \qquad (1) \end{aligned}$$

where

$$H_0 = h\nu/g\beta,\ g^2 = g_{\perp}{}^2 + (g_{//}{}^2-g_{\perp}{}^2)z^2$$

and

$$K^2g^2 = A_{//}{}^2g_{//}{}^2z^2 + A_{\perp}{}^2g_{\perp}{}^2(1-z^2).$$

In the limiting case of $z=\cos\delta=1$,

$$\begin{aligned} H(m_I) = H_{//} - (A_{//}m_I/g_{//}\beta) \\ - (2H_{//})^{-1}\cdot(g_{//}\cdot\beta)^{-2}\cdot A_{\perp}{}^2\cdot\{I(I+1)-m_I{}^2\}, \qquad (2) \end{aligned}$$

can be derived. The positions of the hf-lines (at any m_I, $m=m_{I1}+m_{I2}$ and $m_{I1}+m_{I2}+m_{I3}+m_{I4}$ respectively),

Table 7. Comparisons of spin concentration of the low-temperature-type spectrum with numbers of SO_3 and SO_2 at 580 °C in equilibrium of SO_2 oxidation

Sample	n_{SO_3} SO_3 mols $\times 10^{19}$	n_{SO_2} SO_2 mols $\times 10^{19}$	n_{spin} Spin concn $\times 10^{19}$	$n_{vanad.}$ Vanadium atom $\times 10^{19}$	$n_{spin}/n_{vanad.}$
S_s-1	1.6	6	0.06	20	0.003
S_s-2	5.6	27	0.05	30	0.0017
S_s-3	0.5	41	0.01	21	0.0005

which were calculated by means of Eq. 2 using the parameters of $g_{//}=1.924$; $A_{//}=8.4$, $A_{\perp}=3.3$ mT and $g_{//}=1.917$; $A_{//}=4.3$ mT, are given above and below the spectra in Figs. 2 and 5 respectively. In the latter case the third term of Eq. 2 is neglected. The parameters are listed in Table 6 for the sake of comparison.

From the discussions both the g-values and the hf-coupling constants, it is clear that the ESR spectra, like what those which have previously been observed in doped and undoped V_2O_5 by many authors,[14–18] can also exist in the highly purified V_2O_5 under the conditions of SO_2 oxidation. The spectra with hfs values of 15 lines and more than 20 lines can, then, be conclusively ascribed to the $V^{4+}\cdots V^{5+}$ and $\begin{array}{ccc} V^{4+} & \cdots & V^{5+} \\ \vdots & & \vdots \\ V^{5+} & \cdots & V^{5+} \end{array}$ sites, produced by the elimination of lattice oxygens without the interpositions of other metal impurities.

Low-temperature-type Spectrum of the V_2O_5 Crystal under the Conditions of SO_2 Oxidation. The thermal analysis of $V_2O_5 \cdot nH_2O$ has been carried out in several atmospheres by many authors.[22–25] From those results, above *ca.* 140 °C $VOSO_4 \cdot 3H_2O$ is known to start to change in air to $VOSO_4 \cdot H_2O$ and above *ca.* 200 °C to anhydrated $VOSO_4$; this will be followed by further decomposition, $VOSO_4 \rightarrow V_2O_5$, on heating above *ca.* 550 °C. On the basis of our present knowledge, the changes in the spectrum from a symmetric and broad type to an asymmetric and sharp one in Fig. 6 seems to correspond to the progress in the dehydration and sintering: $VOSO_4 \cdot 3H_2O \rightarrow VOSO_4$. It is known from the suggestion by Ballhausen *et al.*[26] and Ladwig[24] that, in $VOSO_4 \cdot 3H_2O$, some of the water molecules remain in the ligand sites and are replaced by SO_4^{2-} ions as the dehydration progresses. Thus, the crystalline-field splittings of the oxovanadium(IV) ion, and thus the g-values, should differ between $VOSO_4 \cdot 3H_2O$ and anhydrated $VOSO_4$, as will be discussed below.

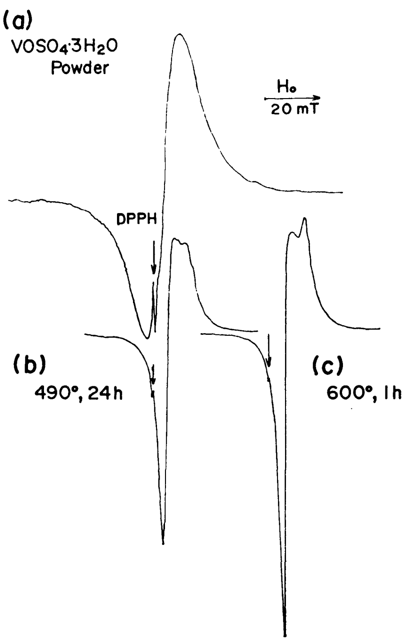

Fig. 6. Changes in ESR spectrum of $VOSO_4 \cdot 3H_2O$ powder with heat treatments, see Table 5.

The rather symmetric line shape of the spectrum of $VOSO_4 \cdot 3H_2O$ might be caused by a similar extent of increase in the linewidth with the anisotropy of the g-tensor of the spectrum of anhydrated $VOSO_4$ in Fig. 6. Such an increase in the linewidth must be due mainly to some effects of the ligand water on the relaxation time.[27] The reason can not be explained fully now, although the fact that the structure,[24,28] linked tightly by SO_4^{2-} tetrahedrons, is realized by the elimination of the ligand water seems to give a hint.

The g-values of powdered $VOSO_4 \cdot 5H_2O$[29] and $VOSO_4 \cdot 2H_2O$[30] have been reported to be $\langle g \rangle = 1.99$ and 1.96 respectively. The tendency for $\langle g \rangle$ to decrease as the dehydration progresses corresponds closely to the results in Table 5. It is shown in the table, that finally, the g-value became close to the value of the low-temperature-type spectrum. Such a decrease in the g-value could be caused by the increase in the covalency of the vanadyl complex due to the replacement of the water molecules in the ligand sites by the SO_4^{2-} ions.[27] By these comparisons, it seems possible to assign the low-temperature-type spectrum under the conditions of SO_2 oxidation to the $VOSO_4$ phase, formed on the V_2O_5 crystalline lattice.

The amounts of SO_3 formed and SO_2 remaining in the equilibrium at 580 °C were roughly estimated from the initial amounts of SO_2 and O_2 and the equilibrium constant of the reaction, $SO_2 + {}^1/_2O_2 = SO_3$. The values are given in Table 7, while the total number of vanadium atoms in the V_2O_5 crystal and the spin concentrations for the low-temperature-type spectrum at 580 °C are given in Fig. 3. By comparing the data, especially between Samples S_S-2 and S_S-3, it can be surmised that n_{spin} decreases with a decrease in n_{SO_3} and inversely with an increase in n_{SO_2}. Thus, the spectrum can be ascribed to the $VOSO_4$ phase; in contrast to this, the possibility of a different assignment to some kinds of reduced vanadium oxides can clearly be ruled out.

Formation of the $VOSO_4$ Intermediate and the Reaction Mechanism of SO_2 Oxidation on the V_2O_5 Crystal. It is known that the $(n_{spin}/n_{vanad.})$ ratio is 1/2000—1/330, as is shown in Table 7. This indicates that the paramagnetic species, ascribed to $VOSO_4$, is formed only in the surface layer of the crystal, even if the reaction is much prolonged. The curves for the increase in intensity of the low-temperature-type spectrum with the time at 470 and 586 °C in Fig. 4 show clearly the existence of a very fast process at the initial stage and a relatively slow process after that. The initial process can be attributed to the growth of the $VOSO_4$ phase on the surface, especially on the (010) plane, and the second process, to the diffusion of the $VOSO_4$ phase into the bulk.

The abrupt increase and decrease in the intensity of the low-temperature-type spectrum near 600 °C seems to occur reversibly in Figs. 3 and 4. The temperature range where the spectrum suddenly disappears may be consistent with the temperature at which the $VOSO_4$ phase in a V_2O_5–SO_2–SO_3–$VOSO_4$ system is decomposed thermally, although the range should change according to the reaction conditions of the SO_2 oxidation on V_2O_5.[31] The disappearance of the spectrum can, therefore, be related to the process of Eq. 3:

$$2VOSO_4 \rightarrow V_2O_5 + SO_3 + SO_2. \tag{3}$$

At low temperatures the SO_2 oxidation reaction on pure V_2O_5 crystal can be expected to proceed through the $VOSO_4$ intermediate as in the following scheme, Eq. 4:

$$2SO_2 + \frac{1}{2}O_2 + V_2O_5 \rightarrow 2VOSO_4 \rightarrow V_2O_5 + SO_3 + SO_2. \tag{4}$$

On the other hand, at high temperatures it would proceed by the participation of the oxygen defect, surrounded equivalently by four vanadium ions on the V_2O_5 surface, as is suggested by the appearance of the spectrum with an hfs of 29 lines.

The findings that the formation and decomposition of the $VOSO_4$ phase in the V_2O_5 crystal occur reversibly and that the surface brilliance of the (010) plane is kept seem to show the possibility of some regular arrangement of the $VOSO_4$ phase on the surface of the V_2O_5 crystal, as was suggested in a previous paper.[17]

References

1) P. Mars and J. G. H. Maessen, *Proc. Int. Congr. Catal., 3rd. Amsterdam*, **1**, 266 (1964); *J. Catal.*, **10**, 1 (1968).

2) G. K. Boreskov, R. A. Buyanov, and A. A. Ivanov, *Kinet. Katal.*, **8**, 153 (1967); G. K. Boreskov, L. P. Davydova, V. M. Mastikhin, and G. M. Polyakov, *Dokl. Akad. Nauk SSSR*, **210**, 626 (1973).

3) A. R. Glueck and C. N. Kenney, *Chem. Eng. Sci.*, **23**, 1257 (1968).

4) H. Livbjerg and J. Villadsen, *Chem. Eng. Sci.*, **27**, 21 (1972).

5) M. Matsui and R. Kiyoura, *Kogyo Kagaku Zasshi*, **40**, 153, 985 (1937).

6) G. K. Boreskov and V. P. Pligunov, *J. Appl. Chem. USSR*, **13**, 653 (1940); *Chem. Abstr.*, **35**, 3396 (1941); E. V. Gerburt-Geibovich and G. K. Boreskov, *Zh. Fiz. Khim.*, **30**, 1801 (1956); *Chem. Abstr.*, **51**, 7818 (1957).

7) H. Kubota, M. Ishizawa, and M. Shindo, *Ryusan*, **12**, 243 (1959).

8) H. Hara, A. Adachi, and N. Kurata, *Kogyo Kagaku Zasshi*, **62**, 669 (1959).

9) P. Jiru, D. Tomkova, V. Jara, and J. Wankova, *Z. Anorg, Allg. Chem.*, **303**, 121 (1960); *Proc. Int. Congr. Catal., 2nd Paris*, **2**, 2113 (1961).

10) G. K. Boreskov, L. P. Davydova, V. M. Mastikhin, and G. M. Polyakova, *Dokl. Akad. Nauk SSSR*, **171**, 648 (1966).

11) V. M. Mastikhin, G. M. Polyakova, Ya. Zyulkovskii, and G. K. Boreskov, *Kinet. Katal.*, **11**, 1463 (1970).

12) R. E. McCarley and J. W. Roddy, *J. Less-Common Met.*, **2**, 29 (1960).

13) J. Haemers, *Bull. Soc. Chim. Belg.*, **79**, 473 (1970).

14) V. A. Ioffe and I. B. Patrina, *Soviet Phys.-Solid State*, **6**, 2425 (1964); *ibid.*, **10**, 639 (1968); L. V. Dmitrieva, V. A. Ioffe, and I. B. Patrina, *ibid.*, **7**, 2228 (1966).

15) J. L. Ragle, *J. Chem. Phys.*, **38**, 2020 (1963).

16) E. Gillis and E. Boesman, *Phys. Status Solidi*, **14**, 337 (1966).

17) Y. Kera and K. Kuwata, *Bull. Chem. Soc. Jpn.*, **50**, 2438 (1977).

18) K. Hirota, K. Kuwata, and Y. Kera, *Bull. Chem. Soc. Jpn.*, **43**, 3017 (1970).

19) H. Tanaka and A. Matsumoto, *Bull. Chem. Soc. Jpn.*, **39**, 874 (1966).

20) G. Sperlich, *Z. Phys.*, **250**, 335 (1972).

21) B. Bleaney, *Philos. Mag.*, **42**, 441 (1951).

22) J. Roch, *C. R. Acad. Sci.*, **249**, 56 (1959).

23) G. Tridot, *Pure Appl. Chem.*, **13**, 543 (1966).

24) G. Ladwing, *Z. Anorg. Allg. Chem.*, **364**, 225 (1969).

25) R. A. Edge, *J. Less-Common Met.*, **18**, 325 (1969).

26) C. J. Ballhausen and H. B. Gray, *Inorg. Chem.*, **1**, 111 (1962); C. J. Ballhausen, B. F. Djurinskij, and K. J. Wastson, *J. Am. Chem. Soc.*, **90**, 3305 (1968).

27) D. Kivelson and R. Neiman, *J. Chem. Phys.*, **35**, 149 (1961).

28) P. Kierkegaard and J. M. Longo, *Acta Chem Scand.*, **19**, 1906 (1965).

29) M. B. Palmer, M. U. Palmer, D. Palumbo, and F. Sgarlata, *Nuovo Cimento*, **3**, 718 (1956).

30) C. A. Hutchison and L. S. Singer, *Phys. Rev.*, **89**, 256 (1953).

31) H. Flood and O. J. Kleppa, *J. Am. Chem. Soc.*, **69**, 998 (1947).